SLS 2.0
Science Case

Gabriel Aeppli and Leonid Rivkin

Swiss Light Source
Paul Scherrer Institut
CH-5232 Villigen

Version 1.01

December 2017

SLS-2

Prof. G. Aeppli and Prof. L. Rivkin

Research Infrastructure Proposal

21st December 2017

Summary

This document describes a Research Infrastructure Proposal for funding by the ETH Domain for the period 2021-2024. It details plans for a major upgrade of the existing Swiss Light Source at the Paul Scherrer Institute to a fourth-generation, diffraction-limited source.

The Swiss Light Source (SLS) has been operational now for over 16 years. In this period, it has spearheaded much groundbreaking research in biomedicine, engineering and the natural sciences, thanks in large part to the excellent performance of the underpinning electron accelerator and storage ring complex. In addition, it has led the world in industrial exploitation, particularly by the pharmaceutical sector, and spawned numerous new companies, including one of the most successful Swiss-technology spinoffs, Dectris. For much of this time, the SLS was a benchmark in regard to how closely its performance matched the theoretical limits defined by its machine parameters. However, with the advent of the next generation of quasi-continuous short-wavelength light sources, called diffraction-limited storage-rings, that yield an emittance and brightness improved by up to two orders of magnitude, it has become imperative to upgrade the SLS (called SLS-2) in like manner.

The SLS-2 upgrade requires a comprehensive rebuild of the storage ring and magnet lattice, resulting in an improvement in emittance and associated increase in brightness by a factor of forty compared to the existing performance in the most commonly used hard x-ray regime. A phased program of upgrades of the beamlines will begin in parallel to optimize exploitation of the ring. This will start in the same funding period, so that Switzerland can continue to lead in the SLS research most immediately and positively impacted by the enhanced brightness offered by the upgrade, such as ptychography (scanning lensless imaging), macromolecular crystallography, and full-field tomography. All of these fields are expected to undergo sea-changes in scope and quality, because ring brightness improvements will be multiplied by photonic instrument advances, to yield data-rate increases of up to four orders of magnitude.

In this manner SLS-2 will maintain the competitive edge of PSI, the ETH Domain, and Switzerland for the next two decades in the most multidisciplinary and sought-after category of large-research facilities.

1. SCIENTIFIC RELEVANCE, STATE OF THE ART AND POTENTIAL

1.1. Introduction

The Paul Scherrer Institute (PSI) is the largest research institute in Switzerland for the natural and engineering sciences. Its three central 'grand challenges' are in human health, energy and the environment, and matter and materials. They address urgent societal demands in the 21st century, including clean and low-cost energy generation, delivery, and consumption; affordable, targeted, and personal medicine to cater to an ageing population; and high-capacity and energy-efficient information technology. All the drivers require an understanding of materials, devices, and biomedical systems on a nanoscale- or atomic level.

Electromagnetic radiation, across the spectrum from radio waves to gamma rays, has been historically, and continues to be to this day, the most ubiquitous probe in the natural sciences for the investigation and understanding of matter. Sources from the mid-infrared through to the soft ultraviolet most often exploit energy-level transitions in atoms, such as in lasers. However, at shorter wavelengths, the interactions between light and matter become so strong that sources based on electrons bound to atoms would rapidly self-destruct. The only way to circumvent this problem is to remove the nuclei from the equation, implying that higher-energy photon sources must use free electrons, whose energy and motion are controlled by electromagnetic fields. Synchrotrons, first tentatively used for this purpose more than half a century ago, are now the modern workhorses for experiments requiring photons with energies between the ultraviolet (starting approximately at 10 eV) and very hard x-rays at over 500 keV.

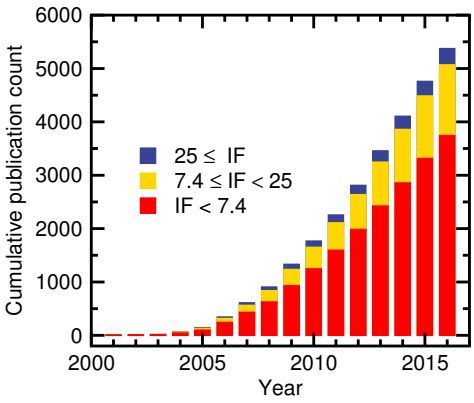

FIG. 1: Cumulative publication record of the SLS from 2001 to end 2016. IF = Impact-factor.

For more than a decade after it delivered 'first light' in 2001, the SLS enjoyed the status of being the benchmark facility for third-generation sources with regards to how close performance matched theoretical limits. From 2006 (when the PSI DUO database was introduced) to the end of 2016, the SLS has been host to 34′578 user visits, 5094 accepted proposals, and 463′304 hours of user beamtime, covering areas as diverse as atomic and molecular science, catalysis/surface science, environmental and earth sciences, condensed-matter physics, life- and medical sciences, materials and engineering sciences, and polymeric- and soft-matter research. Between 2001 and the end of 2016, research output has produced 5373 peer-reviewed papers (see Figure 1), including many high-profile articles [1334 between the impact-factor of Physical Review Letters (7.4) and below that of Science (25), and 298 with an impact-factor of Science and higher]. More than 5000 macromolecular structures solved at the three 'PX' beamlines have, since 2002, been deposited in the Protein Data Bank; in the number of deposited structures per beamline per year, the SLS is the world leader, at 120. A further 15'000 structures of protein/ligand complexes have been determined by industry, many of which have helped the development of drugs under clinical trials to treat ailments such as diabetes, heart disease, and cancer. Technology transfer from SLS has resulted in successful spinoffs such as Dectris and gratXray, both of which have won prestigious national awards in 2017.

In the last decade, however, newer facilities, profiting in part from innovations introduced by the SLS (as did the SLS from earlier facilities), began to achieve similar specifications. Moreover, a new generation of electron storage rings is emerging, that yield an emittance in the horizontal plane two orders of magnitude smaller than previously attainable[1]. The first of these so-called 'diffraction-limited storage rings' (DLSRs) are now beginning to come online. Several more, including SLS-2, the proposed upgrade of SLS detailed in this document, are presently being designed or constructed (Figure 2). The improved brightness of

DLSRs promises paradigm shifts in many synchrotron-radiation-driven scientific disciplines, most notably in imaging, structural biology, and spot-scanning techniques[2]. The need to upgrade the SLS to DLSR status in this highly competitive field has thus become still more urgent. Moreover, the upgrade is most timely, as it will subsume the maintenance and replacement of ageing components of the SLS that are urgently required.

1.2. Scientific justification

The future scientific mission of photon science at the SLS-2 will have its foundations firmly based on already established fields of excellence at PSI. Among others, the SLS to date has produced world-leading research in activities as varied as ptychography, native-SAD, full-field tomography, soft x-ray ARPES, and resonant inelastic x-ray scattering. All these techniques will profit considerably from the upgrade.

Through continuing dialogue with the SLS-beamline staff, presentations to, and feedback from, the PSI Photon-Science Advisory Committee (P-SAC, November 2016, December 2017), the board of the ETH Domain (April 2017), and an international workshop involving users and SLS staff alike (April 2017), a science case tailored around the Swiss and SLS-user international community has been compiled and is summarized here.

The strategy for the upgrade is first to ensure that all beamlines perform at least as well as prior to the upgrade; an initial selection of three beamlines will be redesigned to maximally exploit the enhanced emittance, while future new scientific directions will be simultaneously explored. A second round of upgrades of other beamlines is planned in 2025 to 2028.

A part of the upgrade program will be the incorporation of the 'Digital Platform Initiative', an element of the 2017 State Secretariat for Education, Research, and Innovation (SERI) strategy document, 'Herausforderungen der Digitalisierung fuer Bildung und Forschung in der Schweiz'[3]. It is planned that the SLS-2 project will spearhead a new age in Swiss large-scale projects of 'digitalization', heralding the widespread use of wireless communication, the 'Internet of Things', and the exploitation of machine learning.

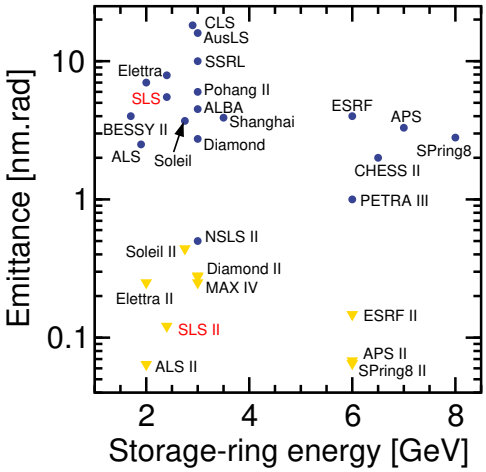

FIG. 2: Emittances of third-generation storage rings (blue circles) and DLSRs (yellow triangles). The SLS and SLS-2 labels are highlighted in red.

1.3. Key science drivers

The enhanced brightness of SLS-2 will benefit almost all the x-ray techniques presently practiced at the SLS. Here, three categories of research activities at the SLS and how these will improve after the upgrade are presented as being particularly illustrative of the sea-changes promised by SLS-2. An exciting aspect is that the improvements extend beyond the increase in brightness alone, due to other innovations downstream from the photon source itself.

1.3.1. Imaging

Imaging at the SLS includes several spectromicroscopies and scanning microspectroscopies, plus full-field tomography and ptychography. The latter two are highlighted here.

Ptychography, a scanning variant of coherent x-ray diffractive imaging, depends intimately on the coherent part of the x-ray beam to encode the necessary information to image objects[6]. It bridges the resolution

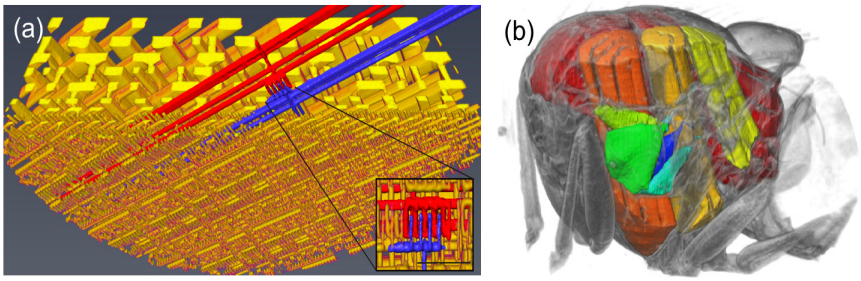

FIG. 3: Examples of imaging research at SLS. (a) Three-dimensional ptychographic tomography of an Intel processor with 15-nm resolution[4]. (b) Cutaway visualization of the thorax of a living blowfly as it beats its wings[5].

gap between crystal diffraction and electron microscopies on the Angstrom and sub-Angstrom scale, and nanoprobe methods such as scanning x-ray transmission microscopy (STXM), photoelectron emission microscopy (PEEM), and tomography on the tens of nanometers to micron scale. Originally developed for electron microscopy, ptychography is now an emerging and increasingly popular and widely adaptable technique using x-rays, largely pioneered at the cSAXS beamline of the SLS. Its great strength is that it can image extended structures with dimensions of several microns and beyond at a resolution of a few nanometers, which makes it ideal for investigating hierarchical structures with nested architectures, not least in complex heterogeneous and biological samples.

A recent ptychography study from the cSAXS beamline reconstructed the internal 3D architecture of an Intel chip with 15-nm resolution [Figure 3(a)] and over a 10-μm-diameter region[4]. This is, to date, unique in being both nondestructive and able to resolve nanoscale elements across distances that are three orders of magnitude larger. Being able to investigate, post-production, a chip in this manner has important implications for the semiconductor industry, regarding both quality control and reverse engineering.

Future chips will continue to have footprints in excess of 1 mm and their design rule will promise to break the 10-nm barrier; ptychographic imaging will thus need to evolve greatly to enable meaningful chip inspection. Radiation from SLS-2 is a precondition for this development, as DLSR-radiation typically contains a two-orders-of-magnitude larger coherent fraction than do hard x-rays produced by third-generation facilities. In addition to the increase in the available coherent flux, further improvements can be brought to bear, including (a) the installation of smaller-period undulators using high-remanence magnetic materials and 'magnetic funnels'; (b) the use of the entire bandwidth of any particular undulator harmonic; and (c) improvements in efficiency of diffractive optics, or the adoption of reflecting optics instead of diffractive Fresnel zone plates, made possible by the smaller footprint of the grazing-incidence beam on the reflecting surfaces. All told, the expected increase in available flux as a result of these enabling technologies is estimated to be in excess of 10000, compared to the current SLS. The proposed improvements in SLS ptychography could also lead to new studies relevant to engineering, including, for example, lock-in studies producing movies of the nanoscale dynamics of engineered magnets[7].

This gain in flux can be invested in one or more of three channels: data-acquisition rates (frame rates and scanning velocities), spatial resolution (scattering vector, Q), and photon energy (which has an impact on the integrated sample dose, particularly important for biological and soft-matter samples), and will be tailored to individual experiments. Moreover, the use of higher photon energies allows one to investigate thicker samples for any given sample material.

Lastly, because the setup for ptychography is so similar to that for STXM, a natural development associated with the SLS-2 upgrade would be to provide soft x-ray ptychography (SXP) in addition to STXM in the range of 250 to 2000 eV, requiring an SXP endstation to operate at an undulator source.

Full-field x-ray computed tomography (XTM) at the 0.1 to 5-micron scale has burgeoned in the last decade and a half, not least in the fields of biological, palaeontological, and industrial imaging [see Fig-

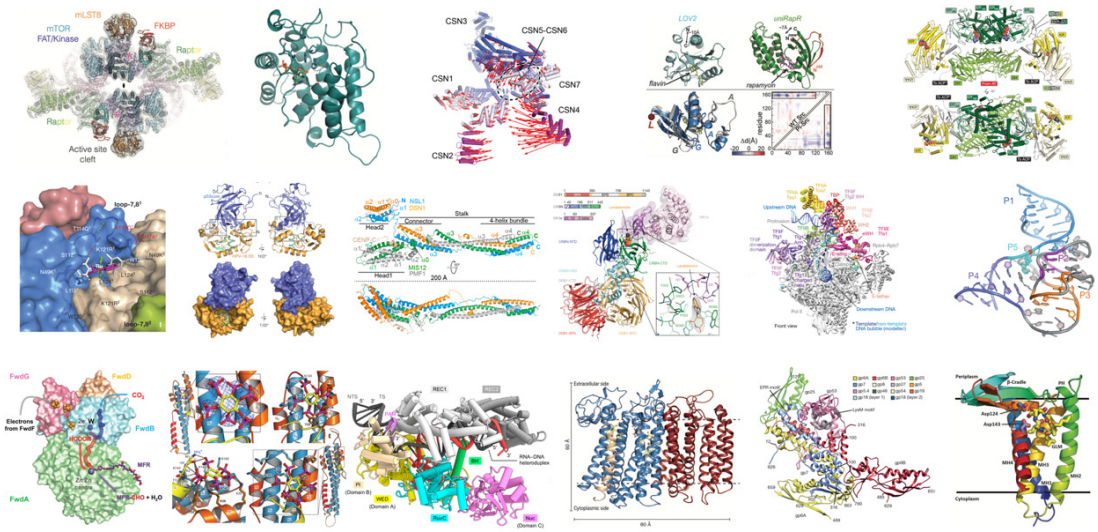

FIG. 4: Examples of biological structures solved at the SLS and published in Cell, Nature, or Science in 2016 alone.

ure 3(b)]. The TOMCAT beamline at the SLS has played a leading role in the development of XTM worldwide since the turn of the century.

The increased brightness from both undulators and high-field superbends at SLS-2 would allow XTM to be performed at much higher energies (with the associated penetration powers and lower integrated doses), and improve dramatically (up to 2000× faster) the dynamic capabilities[5], potentially revolutionizing our understanding of countless life-science, industrial and advanced-manufacturing processes.

Phase-contrast XTM has proved to be especially powerful for low-dose experiments of weakly absorbing biological samples in the hard x-ray regime, not least in the neurosciences – the transverse coherence function of SLS-2 will be significantly more isotropic (i.e., the beam will be rounder). This will facilitate homogeneous edge-enhancement, and should thereby enable more sophisticated reconstruction algorithms that go beyond a linear approximation, which presently only makes use of the first-edge interference fringe. The significantly larger brightness will enable full-field time-resolved imaging at the 100-nm scale with zoom-in capabilities into dedicated regions of interest, thanks to Fourier ptychography. SLS-2 is therefore expected to strongly benefit phase-contrast imaging in all the variants offered at the SLS, including omnidirectional interferometry and full-field Zernike techniques[8].

1.3.2. Molecular biology

Light sources have revolutionized modern macromolecular crystallography (MX). To date, well over 120'000 atomic-resolution structures have been deposited in the Protein Data Bank (www.pdb.org). The MX groups at SLS are among the most successful worldwide, providing, for example, crucial data that resulted in the 2009 Nobel Prize in Chemistry for the structure and function of the ribosome[9].

However, one important class of protein, membrane proteins, including their subclass, G-protein-coupled receptors (GPCRs), which accounts for one third of all proteins and two thirds of medicinal drug targets, is extremely under-represented (1 - 2%). This is in a large part due to their hydrophobic nature, which makes crystallization difficult and normally limits crystal sizes to the micron scale. Such crystals require micron- or submicron beam focussing, which, until the advent of DLSRs, meant divergences in the horizontal plane that weakened the diffraction signal at high resolution. Most membrane proteins are relatively small – for example, GPCRs are almost all under 40 kDa, excluding them from investigation using cryo-EM. Even molecules up to 250 kDa can, in almost all cases, only be investigated via cryo-EM with

a resolution that is insufficient for atomic-scale studies. MX at SLS-2 will therefore concentrate on such systems, individually tailoring case-for-case the division of the improved emittance between divergence and focus size.

Due to radiation damage, individual microcrystals are insufficient for a complete data set, hence diffraction data from multiple crystals are merged[10]. Prompted by successes in serial femtosecond crystallography (SFX) at XFELs, there has been a thrust in the last five years towards similar approaches using synchrotron radiation in a technique coined synchrotron serial crystallography (SSX)[11]. SSX can be carried out at room- and cryogenic temperatures alike, requiring novel approaches to sample preparation, delivery, data collection, and processing.

Room-temperature MX is experiencing a renaissance through SSX. Despite the one to two orders of magnitude reduction in the highest tolerable dose compared to cryo-MX, RT-SSX offers several advantages, including sampling conformational landscapes, dispensing with cryoprotectants, and, crucially, investigations of dynamic processes down to the microsecond time-scales[12]. Moreover, and importantly with regards to the tight but quasiparallel focusing attainable at SLS-2, it has been demonstrated that, in contrast to cryo-MX, there is a positive correlation between dose rate and maximum tolerable integrated dose in RT-SSX, which enables the measurement of more useful diffraction data by approximately a factor of six when increasing the dose rates from 0.5 to 5 MGy/s[13].

In a very recent study performed at the SLS, the structures of the human adenosine A_{2A} GPCR ($A_{2A}R$), and the αβ-tubulin-darpin complex (TD1) have been determined using RT-SSX to a resolution of 2.1 Å[14], revealing unexpected differences between cryo- and room-temperature structures around the ligand-binding site of TD1, indicating that room-temperature structures may provide additional information about protein dynamics for ligand binding.

$A_{2A}R$ is exceptional for a membrane protein in that relatively large and well-diffracting crystals can be grown (the above study used crystals as large as 30 μm), making its study amenable to third-generation sources. No such luxury will be afforded to the large majority of the as-yet unstudied membrane proteins, which typically only produce weakly diffracting crystals with dimensions of the order of a few microns or still smaller. For these studies, the high brightness and small, parallel, beam of SLS-2 will be crucial in enhancing signal-to-noise ratios and reducing sample consumption.

SSX will thus function far more efficiently and allow a whole vista of new macromolecules to be investigated with the micron- and submicron-sized parallel beams promised by SLS-2. Since many membrane proteins are expected to be novel, experimental phasing is required to reveal their structures. The recent progress in native-SAD phasing (in which the PSI is a leading player) has led to great advances in *de novo* phase determination[15]. SLS-2 will provide a timely opportunity to optimize existing MX beamlines for native-SAD experiments, which require x-rays down to 3 keV and sample environments with minimum background scattering and absorption[16].

Still higher photon intensities are possible by increasing the relative bandwidth of the incident monochromatized radiation. Except for the very largest-unit-cell samples, an increase in bandwidth, and hence also photon-delivery rates, by a factor of 10 through the use of multilayer monochromators, could be easily tolerated. Combined with detectors capable of frame-rates of hundreds of Hz, SSX at SLS-2 will not only enable biologists to study structure and function of largely unexplored protein families, but also pave the way for high-throughput, structure-based, drug discovery of membrane proteins, an application entirely unsuited to cryo-EM, but one that will become still more central to MX as the realm of membrane proteins and GPCRs begins to reveal itself.

RT-SSX allows dynamic studies down to the microsecond scale or even shorter. Cryo-EM can only freeze proteins as they undergo conformational changes, and is limited to temporal resolutions of the order of a tenth of a second. Moreover, dynamical studies in cryo-EM typically involve movements of large portions of a protein; it is incapable of resolving subtle but decisive local changes, such as in the studies of TD1. The better signal-to-noise ratio and the higher throughput of SSX at SLS-2 will be the key to unlocking the full potential of time-resolved studies. SSX, in combination with complementary XFEL

studies, will thus continue to be the only reasonable techniques for protein dynamics on the millisecond to femtosecond timescale.

1.3.3. X-ray spectroscopies

Most x-ray spectroscopies will profit from the smaller focal spots possible at SLS-2. At a typical undulator beamline, the horizontal source size will be approximately a factor of six smaller than at present. As the divergence is also approximately eight times smaller, the beam footprint in the x direction will be correspondingly smaller; focussing optics can thus be positioned significantly further downstream, enabling more extreme demagnification and a more efficient use of circular diffraction-based optics such as FZPs. This will allow bulk investigations using soft x-ray ARPES with nanofocussing, and *operando*-characterization of devices and heterogeneous materials[17,18] (see Figure 5).

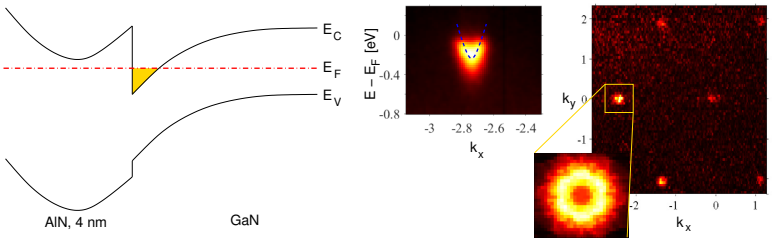

FIG. 5: SX-ARPES of quantum-well states in a AlN/GaN heterostructure, recorded at 1250 eV. The high gradient of the parabolic band structure indicates a high mobility electron gas, with an effective mass of 0.25 m_e. From[18].

Resonant inelastic x-ray scattering (RIXS) is a rapidly developing experimental method in which photons resonant with electronic transitions are inelastically scattered[19]. The energy loss between the scattered and incident photon (from meV to a few eV), plus the momentum transfer and change in polarization between the incoming and outgoing photon, can be directly associated with important processes underpinning emerging properties such as superconductivity, charge-density waves, and magnetism.

The energy resolution in RIXS is determined largely by the spot size on the sample in the dispersive direction of an analysis grating spectrometer. The tighter focal spot size of DLSRs will correspondingly improve the performance, which will be further enhanced at SLS-2 by extending the beamline by over a factor of two to approximately 100 m, and increasing the demagnification. In this manner, sub-10-meV resolution should be obtained, with the option of domain raster-scanning with submicron-sized beams on the sample and enabling the possibility of following, among other things, *operando* magnetic- or ferroelectric-domain switching.

Another interesting concept is to disperse the incident radiation from the grating monochromator and project this onto the sample. Perpendicular to the dispersed incident beam, the focus remains tight, thereby preserving the resolution. By then dispersing the scattered radiation with a second grating, the image formed on an area detector allows the parallel detection of both the incident- and inelastically-scattered spectra in orthogonal directions[20], enabling efficient, high-resolution, time-resolved experiments.

RIXS can also be performed in the tender x-ray regime (2 to 4 keV) to access the L-edges of the ruthenates (exploring Mott physics and potential topological superconductivity and its relation to spin-orbit interactions) and M-edges of the actinides (to investigate, again, unconventional superconductivity and the competition between itinerant and localized $5f$-electrons and crystal-field effects). An extension of the photon-energy range of the RIXS beamline at SLS-2 to 4 keV would thus be highly advantageous.

Hard x-ray scanning spectroscopies will also profit from the tight focus possible at SLS-2. Moreover, line tomographies (which involve two transverse scanning coordinates and one rotational coordinate) will, like MX, take advantage of both tight and parallel beams[21] down to the submicron scale. These ‘chemical imaging’ techniques exploit one or more of several signals (e.g., fluorescence, XANES, XRD) simultaneously, and can be applied to disciplines as broad as art history, cultural heritage, heterogeneous catalysis,

battery technologies, and environmental sciences.

1.4. Upgrade of the machine to a DLSR

The machine conceptual design report, which was presented to the Machine Scientific Advisory Committee in September 2017 and very favourably received (see also the letter from the MSAC Chairman attached in this proposal), is provided as an Appendix in this proposal submission[22] and at the link `http://ados.web.psi.ch/SLS2/CDR/Doc/cdr.pdf`.

The original SLS storage ring contains 12 triple-bend achromats (TBAs), has a circumference of 288 m, and provides an emittance of 5 nm at 2.4 GeV.

The upgrade to DLSR status had to address the issue of the comparatively small ring circumference, because, as a rule of thumb, emittance scales approximately inversely with the third power of the number of lattice cells (i.e., bending magnets with adjacent quadrupoles for focusing) installed along the machine circumference. In the new generation of multibend-achromat (MBA) lattices, this number was increased through miniaturization of all components. Nonetheless, scaling existing DLSR designs (MAX-IV, SIRIUS, ESRF-EBS, etc.) to the circumference and energy of the SLS was insufficient to provide the desired emittance reduction; thus, a novel type of lattice was developed.

The emittance in a storage ring is determined by the equilibrium between radiation damping and quantum excitation. The latter depends on the strength of the magnetic field and on the magnitude of the dispersion function, because an electron starts to oscillate after emission of a photon around the closed orbit corresponding to its reduced energy. Quantum excitation is minimized by using so-called longitudinal gradient bends (LGBs), bending magnets for which the field varies and steeply peaks along the beam path; and by minimizing the dispersion function at the LGB center, where the field is strongest. Complete dispersion-suppression is achieved by means of so-called reverse bends (RBs), small bending magnets of opposite field polarity realized by transverse displacement of the horizontal-focusing quadrupoles in order to obtain the desired dipolar down-feed. Moreover, radiation damping is also enhanced, because the field variation in the LGB increases the radiated power compared to a homogeneous bending magnet, and the total absolute bending angle of the lattice is larger than 360^{o}, due to the negative bending of the RBs. Furthermore, the quadrupole component in the RBs redistributes damping in favour of the horizontal dimension. Altogether, the LGB-RB MBA lattice cell provides almost a five times lower equilibrium emittance compared to a conventional one. This is an innovative and unique feature of SLS-2.

In the new lattice, the existing 12 TBAs of three different types will be replaced by 12 identical 7-bend achromat arcs (7BAs) made from five full and two half LGB-RB cells. All 12 straight sections will be 5.5 m long. Eight full-straights and three half-straights are available for undulator installation, the others being required for injection elements and RF cavities. The higher lattice symmetry compared to SLS necessitates modifications of the lattice footprint, mainly affecting the regions of the present 'long' straights, while moderately affecting the others. A comparison of the most important lattice parameters of SLS and SLS-2 is given in Table I. Figure 6 also highlights the much cleaner spectra of SLS-2. For both rings, the beam energy is 2.4 GeV and the stored current 400 mA. The SLS lattice is given in its present configuration, including three 2.9-T superbends and the chicane for laser-beam slicing (FEMTO), which will not be part of SLS-2. Three longitudinal gradient super-bends of 6-T peak-field are included in the SLS-2 lattice.

Optimization of the dynamic acceptance is one of the most challenging problems for any low-emittance lattice – the small dispersion requires very strong sextupoles for chromaticity correction. Fortunately, the cell tune where the RBs most efficiently suppress the LGB dispersion is also well suited to establish a basic resonance-cancellation due to the periodic structure of the 7BA arc. Fine-tuning several sextupole and octupole magnets provided further optimization. In this manner, sufficient acceptance was obtained to predict a beam lifetime of about 9 hours (similar to SLS now), and enable off-axis injection from the existing SLS booster ring. This latter was an innovative design at its time, later adopted at several other

Parameter	SLS	SLS-2
Circumference [m]	288.0	290.4
Total absolute bending angle [°]	374.7	561.6
Horizontal emittance [pm]	**5630**	**126**
Energy spread [$\times 10^{-3}$]	0.86	1.07
Radiated power [kW]	219.5	221.6
Momentum compaction factor α [$\times 10^{-4}$]	6.04	-1.33
Enhancement of horizontal damping (J_x)	1.00	1.71
Coherent fraction @ 10 keV, 2-m undulator	$\mathbf{1.4 \times 10^{-3}}$	$\mathbf{6 \times 10^{-2}}$

TABLE I: Machine parameters for SLS and SLS-2.

sites. It delivers a comparatively low emittance of 10 nm, making it suitable for injection into SLS-2.

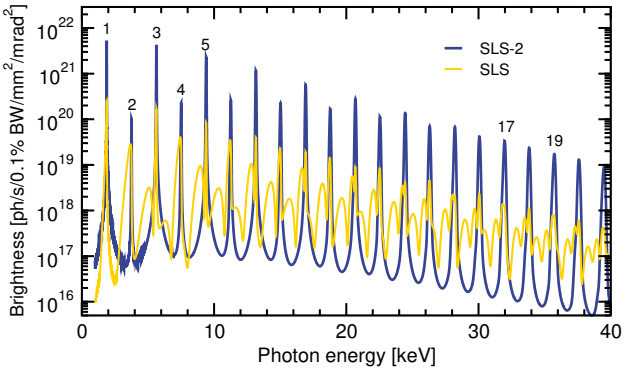

FIG. 6: Comparison of a U12 undulator brightness spectrum inserted at the SLS and SLS-2, all other conditions being equal ($K = 1.6$, 240 poles).

For top-up injection, the novel 'anti-septum' scheme was developed. It is based on a conventional orbit bump formed by three dipole kickers, where the middle kicker contains a current sheet, screening the injected beam from the kicker field, thus forming the anti-septum. This sheet can be made rather thin, thus reducing the distance between stored and injected beam and with it, the aperture requirements. More advanced schemes, which enable on-axis injection, are also under development.

The vacuum chamber is based on a round beam pipe of 20 mm diameter. Sections with antechambers in the LGB regions, where radiation is emitted at high power, alternate with sections made from simple round pipes in the RB regions. Most of the inner surface of the vacuum chamber is coated with nonevaporable getter (NEG) material, in order to establish a low average pressure of $< 10^{-9}$ mbar after 100 Ah of beam dose. Calculations of the vacuum-chamber impedance and simulations of beam instabilities predict that the desired beam current of about 1 mA per bunch (400 mA total current) can be safely stored.

Small apertures are a basic feature of DLSR lattices, because they enable an increase of magnet gradients and thus a reduction of magnet length and miniaturization of lattice cells. For the SLS-2 magnets, resistive coil (RC) and permanent magnet (PM) designs are being evaluated in parallel, the final decision depending on costs and ongoing technological progress in the field. The main component is a compound magnet containing the central LGB with about 2-T peak field and two vertically focusing combined-function bending magnets (VB). Any of these may be exchanged by a superconducting LGB enclosed by two separate VBs.

The magnets are mounted on girders supported by concrete pedestals, to provide maximum stability. Depending on the elements they carry, these supports will be equipped with motorized movers for remote alignment, or with simple manual adjustments. Regardless of the final decision on the girder layout and adjustments, which will also be cost driven, the mechanical tolerance and stability requirements with regards to beam-dynamics performance can be met, and it is the subject of ongoing studies as to what extent remote alignment capabilities may shorten the commissioning period and facilitate operation.

Expt/source	Figure of merit	Factor improvement SLS-2/SLS	Comment
Ptychographic	Resolution [nm]	10^4: 14 $\rightarrow$ 1.4 ($I \propto Q^{-4}$)	Experiment described in Reference[4].
tomography, 6.2 keV,	Probed volume [μm^3]	10^4: 1800 $\rightarrow 1.8 \times 10^7$	
cSAXS	Time	10^4: 22 h $\rightarrow$ 8s	Change only one parameter
Scanning SAXS	Size sensitivity [nm]	10^3: 50 $\rightarrow$ 8	Experiment described in Reference[23].
tomography, 12.4 keV,	Probed volume [μm^3]	10^3: 2.5 $\rightarrow$ 2500	
cSAXS	Time	10^3: 22 h $\rightarrow$ 80s	Change only one parameter
Tomography,	Spectral flux	0.91 @ 10 keV; 1.35 @ 20 keV	Incident on 1 mm^2 @ 25 m
5.4-T superbend	[ph/s/0.1% BW]	3.1 @ 40 keV; 16.0 @ 80 keV	
	Flux	0.91 @ 10 keV; 1.35 @ 20 keV	Incident on 1 mm^2 @ 25 m
	[ph/s]	3.1 @ 40 keV	MML: $\Delta\nu/\nu = 0.02$
Tomography,	Spectral flux	9400 @ 10 keV; 1850 @ 20 keV	Incident on 1 mm^2 @ 25 m
U12 undulator	[ph/s/0.1% BW]	350 @ 40 keV	
	Flux	2300 @ 10 keV; 460 @ 20 keV	Incident on 1 mm^2 @ 25 m
Tomography	[ph/s]	90 @ 40 keV	MML: $\Delta\nu/\nu = 0.005$
MX,	Brightness	75 @ 6 keV; 105 @ 12 keV;	Multiply increase further by ~ 10 when
U14 undulator	[ph/s 0.1%BW mm^{2}mr^2]	175 @ 16 keV	using full harmonic content
nano-SX-ARPES	Focus @ sample	$74 \times 10 \rightarrow 0.2 \times 0.2$ μm^2 (18'500)	Up to 2 keV
@ ADRESS, U33			
nano-RIXS	Focus @ sample	$52 \times 4 \rightarrow 0.2 \times 0.2$ μm^2 (5'200)	No spectral distortions expected for
@ ADRESS, U33			metals due to charging

TABLE II: Expected improvements in performance at selected experiments at SLS-2.

2. USES, FUNCTION, ACCESS

SLS-2 will operate in the manner which has succeeded for SLS. The SLS has been an open-access, peer-review-based user facility (see the PSI DUO website https://duo.psi.ch/duo/) and follows an open-data policy. As well as free-of-charge, open-access experiments (approximately 4000 user visits per year), proprietary (costed) research is carried out at several beamlines, most notably PX and Materials Science, through SLS Techno-Transfer AG (SLS-TTAG). The process leading to beamtime allocation includes checks for safety and ethics.

The scientific usage of SLS-2 will both continue to cater for the well-established community of the existing machine in all the scientific fields listed in Section 1.1, and should also attract new users across a broad spectrum of disciplines, particularly in the life sciences and imaging, be it for biological samples, industrial components, or cultural artefacts, to name just three examples. Access will continue to be through bi-annual external peer-reviewed proposal submissions. Typically, beamtimes occur within continuous 24-hour operations for six days per week, interspersed every five to six weeks with shutdowns for machine maintenance.

3. SCIENTIFIC AND TECHNICAL FEASIBILITY

Table II provides an overview of the expected improvements of SLS-2 at highlighted experiments.

PSI is in close contact with the first greenfield DLSRs, MAX-IV in Lund, Sweden (inaugurated in 2016) and Sirius in Campanas, Brazil (expected 2019), as well as the well-advanced ESRF 'EBS' upgrade, plus several more at earlier stages of the upgrade process (in particular the APS in Argonne, USA, and the ALS at Berkeley). Continued dialogue with the DLSR-community will assist in minimizing unforeseen

obstacles. Detector development at PSI continues apace, especially with regards to automatic gain-adjusting integrating detectors such as the 'Jungfrau'.

The feasibility of the lattice design was very positively evaluated by the Machine Conceptual-Design-Review Panel in September 2017. The next step is to produce a detailed Technical Design Report (TDR), which will be the basis for the procurement of the accelerator systems. The TDR work will be completed by mid 2019 and cover detailed specifications, prototype development, as well as a design of a full achromat mock-up. In this manner, any obstacles should be identified and solved far in advance of the actual upgrade procedure. In parallel, beamline components, including novel sources (in particular short-period undulators and LG-superbends), the front-end, and x-ray optics, are already being evaluated to ensure performance is maintained across the board, and to facilitate the design of the first phase of beamlines that will actively exploit the enhanced performance of the SLS-2 machine.

The 'dark period' between the last experiment of the existing SLS and the first pilot experiments at SLS-2 is planned to last 18 months, beginning in April 2023. To complete the significant civil-engineering tasks associated with removal of the old lattice and installation of the new machine within this allotted period, many of the new components will be fabricated and tested *ex situ* in advance so that they can be introduced and interfaced swiftly and efficiently.

During the upgrade, machine implementation will be led by the Large-Research Facility (GFA, Professor Leonid Rivkin) Division of PSI, while the installation of sources and upgrades to the beamlines will be managed by the Photon-Science Division (PSD, Professor Gabriel Aeppli). Both exercises will involve close collaboration between GFA and PSD, taking full advantage of the Logistics and Accelerator Divisions at PSI, as well as the recent experience of successful SwissFEL construction and commissioning by the same staff which will be responsible for SLS-2. The PSD develops and operates all aspects of SLS and SwissFEL photonics from conventional gun and pump lasers, through undulators, to beamlines and analysis software, including underpinning technology (e.g., optical elements and detectors), in-house scientific exploitation and external user programs.

4. CONCLUDING REMARKS

Electron-driven photon sources have a remarkable track record in science, technology and biomedicine. The underlying physics as well as a demand for seeing matter at the nanoscale ensure that they will continue to be essential for scientific and technical progress in the future. Therefore, most third-generation electron storage rings are either considering or actively undergoing an upgrade to DLSRs. It is imperative that the SLS does likewise. Novel machine elements pioneered at the PSI, in particular reverse-bend dipoles and longitudinal-gradient bends, enable an approximately factor of forty improvement in horizontal emittance, despite the small ring circumference. This will maintain the pre-eminence of PSI, the ETH Domain, and Switzerland in photon science, which has been established by the current SLS and SwissFEL for the foreseeable future (Figure 2).

The beamline upgrades will be in two phases. The first phase, in parallel with the machine upgrade, will encompass those beamlines most positively impacted by the increased brightness, probably including ptychography, full-field tomography, macromolecular crystallography, soft x-ray ARPES, and resonant inelastic x-ray scattering. We anticipate that the design, construction and exploitation of SLS-2 will enable not only advanced research and education, but also the continued excellence of technology transfer demonstrated by SLS-1, especially in partnership with InnovAare, the node of the Swiss Innovation Park to be located next to SLS-2.

[1] Electron storage rings simultaneously provide many beams of radiation characterized by high fluxes (F), small source sizes (σ), and high collimation (σ'). The standard figure of merit for synchrotron radiation encapsulating these properties is the so-called **brightness**, given by $B = F/(\sigma\sigma')$. The product of the source size and divergence $\sigma\sigma'$ is called the **emittance**, which should thus be designed to be as small as possible.

[2] E. Weckert, IUCrJ **2**, 230 (2015).

[3] https://www.sbfi.admin.ch/sbfi/de/home/aktuell/medienmitteilungen.msg-id-67456.html . (2017).

[4] M. Holler, M. Guizar-Sicairos, E. H. R. Tsai, R. Dinapoli, O. Bunk, J. Raabe, and G. Aeppli, Nature **543**, 402 (2017).

[5] S. M. Walker, D. A. Schwyn, R. Mokso, M. Wicklein, T. Müller, M. Doube, M. Stampanoni, H. G. Krapp, and G. K. Taylor, PLOS Bio. **12**, e1001823 (2014).

[6] H. M. L. Faulkner and J. M. Rodenburg, Phys. Rev. Lett. **93**, 023903 (2004).

[7] C. Donnelly, M. Guizar-Sicairos, V. Scagnoli, S. Gliga, M. Holler, J. Raabe, and L. J. Heyderman, Nature **547**, 328 (2017).

[8] G. Zheng, R. Horstmeyer, and C. Yang, Nature Photonics **7**, 739 (2013).

[9] M. Selmer, C. M. Dunham, F. V. Murphy IV, A. Weixlbaumer, S. Petry, A. C. Kelley, J. R. Weir, and V. Ramakrishnan, Science **313**, 1935 (2006).

[10] J. L. Smith, R. F. Fischetti, and M. Yamamoto, Curr. Op. Struct. Biol. **22**, 602 (2012).

[11] K. Diederichs and M. Wang, Methods Mol. Biol. **1607**, 239 (2017).

[12] V. Panneels *et al.*, Struct. Dyn. **2**, 041718 (2015).

[13] R. L. Owen, N. Paterson, D. Axford, J. Aishima, C. Schulze-Briese, J. Ren, E. E. Fry, D. I. Stuart, and G. Evans, Acta Cryst. D **70**, 1248 (2014).

[14] T. Weinert *et al.*, Nat. Comms. **8**, 542 (2017).

[15] Q. Liu and W. A. Hendrickson, Curr. Op. Struct. Biol. **34**, 99 (2015).

[16] A. Wagner, R. Duman, K. Henderson, and V. Mykhaylyk, Acta Cryst. D **72**, 430 (2016).

[17] V. N. Strocov, M. Kobayashi, X. Wang, L. L. Lev, J. Krempasky, V. V. Rogalev, T. Schmitt, C. Cancellieri, and M. L. Reinle-Schmitt, Synch. Rad. News **27**, 31 (2014).

[18] L. L. Lev, I. O. Maiboroda, E. S. Husanu, M.-A. Grichuk, N. K. Chumakov, I. S. Ezubchenko, X. Wang, T. Schmitt, M. L. Zanaveskin, V. G. Valeyev, and V. N. Strocov, Under review.

[19] L. J. P. Ament, M. van Veenendaal, T. P. Devereaux, J. P. Hill, and J. van den Brink, Rev. Mod. Phys. **83**, 705 (2011).

[20] V. N. Strocov, J. Synch. Rad. **17**, 103 (2010).

[21] C. Corkhill, D. Crean, D. Bailey, C. Makepeace, M. Stennett, R. Tappero, D. Grolimund, and N. Hyatt, Nat. Mat. Degrad. **1**, 19 (2017).

[22] A. Streun (Ed.), *SLS-2 Conceptual Design Review, PSI Bericht 17-03* (2017), Appendix, this proposal, and http://ados.web.psi.ch/SLS2/CDR/Doc/cdr.pdf .

[23] M. Liebi, M. Georgiadis, A. Menzel, P. Schneider, J. Kohlbrecher, O. Bunk, and M. Guizar-Sicairos, Nature **527**, 349 (2015).